ORIGIN OF THE SPINEL-PYROXENE SYMPLECTITES IN THE HARZBURGITES FROM THE NEW CALEDONIA PERIDOTITE

Arianna Secchiari*, Alessandra Montanini*, ✉, Delphine Bosch**, Patrizia Macera*** and **Dominique Cluzel°**

* *Dipartimento di Scienze Chimiche, della Vita e della Sostenibilità Ambientale, Università di Parma, Italy.*
** *Geosciences Montpellier, Université de Montpellier, France.*
*** *Dipartimento di Scienze della Terra, Università di Pisa, Italy.*
° *Institut des Sciences Exactes et Appliquées, Université de la Nouvelle-Calédonie, New Caledonia.*
✉ *Corresponding author, email: alessandra.montanini@unipr.it*

ABSTRACT

The New Caledonia ophiolite (Peridotite Nappe) hosts one of the largest and best-exposed mantle section worldwide, providing an exceptional insight into upper mantle processes. The Peridotite Nappe is mostly dominated by harzburgites, locally overlain by mafic-ultramafic cumulates, but also includes minor spinel and plagioclase lherzolites, cropping out in the northern part of the island.

The New Caledonia harzburgites are low-strain tectonites, showing dominant porphyroclastic textures. The main mantle paragenesis is constituted by olivine (~ 75-85 vol%), orthopyroxene (~ 15-25 vol%) and spinel (< 1 vol%), while primary clinopyroxene is notably absent. An important textural feature of these mantle rocks is represented by the common occurrence of spinel-pyroxene symplectitic aggregates.

In this work, we present a petrographical, textural and major element chemical characterization of the spinel-pyroxene symplectitic intergrowths occurring in the New Caledonia harzburgites (Kopeto, central massif, and Yaté, Massif du Sud). Based on textures, size and relationships with the other mineral phases, these spinel-pyroxene clusters have been divided into two types, named type-A and type-B.

Type-A symplectites occur in the Kopeto harzburgites and are composed of spinel-orthopyroxene (± clinopyroxene) intergrowths. In type-A symplectites, symplectitic spinel (Spl 2) occurs as abundant vermicular shaped grains, ranging in size from ~ 0.5 to 2 mm. By contrast, spinel of the porphyroclastic assemblage (Spl 1) shows smaller size (in the range of few µm) and notably lower abundances (< 1%). Type-A symplectites develop exclusively on porphyroclastic olivine, which in turn displays evidence of chemical disequilibrium and corroded outlines.

Bulk major element compositions reconstructed for type-A symplectites rule out a derivation from a pre-existing garnet phase, as the model garnet compositions do not satisfy garnet stoichiometry, being characterized by Si deficiency. By contrast, major element chemical variations of the symplectitic phases, coupled with the high abundance of Spl 2 and olivine resorption, suggest an origin from reactive percolation of opx-saturated hydrous melts or slab-derived fluids in a subduction zone setting.

Type-B symplectites are found in Yaté sample and consist of spinel-orthopyroxene (± clinopyroxene). They are characterized by smaller size (few hundreds of µm, i.e. "micro-symplectites") and different shapes compared to type-A symplectites, growing as vermicular, "myrmekite-like" intergrowths at the rims of porphyroclastic orthopyroxene. Major element chemical compositions of type-B symplectites are consistent with an origin as "cooling textures". These structures may derive from unmixing of a high-T, Al-Cr rich, orthopyroxene due to the decreased solubility of the Cr-Al component (CrMgTs) during post-melting lithospheric cooling at T < 900°C.

INTRODUCTION

Symplectites are complex vermicular ("worm-like") intergrowths of different mineral phases, often observed in metamorphic and igneous rocks (Vernon, 2004). In mantle lithologies, the presence of spinel-pyroxene symplectites has been widely documented and the origin of these structures was ascribed to various processes (e.g. Smith, 1977; Field and Haggerty, 1994; Godard and Martin, 2000; Seyler et al., 2007; Rampone et al., 2008; Shimizu et al., 2008).

On the basis of major element compositions, spinel-pyroxene clusters have been often interpreted as breakdown products of garnet (e.g. Vannucci et al., 1993; Medaris et al., 1997; Morishita and Arai, 2003; Rampone et al., 2009). Different authors have indeed demonstrated that mass balance calculations on bulk symplectites match garnet stoichiometry and hence spinel-pyroxene intergrowths have been referred as a clue of a pre-existing garnet phase (e.g. Takahashi, 2001; Shimizu et al., 2008). By contrast, garnet signature is rarely preserved by trace element chemistry in symplectitic domains (e.g. Morishita and Arai, 2003).

Another explanation proposed for mantle symplectites includes origin through melt-rock reactions and precipita-

tion of mineral phases from a melt (e.g. Seyler et al., 2007; Suhr et al., 2008; Godard et al., 2008). Similar structures have been recognized in Mid Atlantic Ridge (MAR) peridotites, where their presence has been ascribed to reactive percolation of MORB-type or alkaline melts, resulting in polyphase precipitation of spinel-orthopyroxene-clinopyroxene intergrowths (Seyler et al., 2007; Suhr et al., 2008).

Spinel-pyroxene symplectitic aggregates have also been interpreted as "cooling textures" generated through unmixing of clino- or orthopyroxene due to decreased solubility of the Cr-Al component (CrMgTs) in pyroxenes and subsolidus Fe-Mg exchange reactions between pyroxenes and spinel at decreasing temperature (e.g. Field and Haggerty, 1994; Rampone et al., 2008).

Finally, hybrid origins, including reaction between a former garnet and percolating fluids during post-melting cooling history, have also been invoked for the genesis of complex symplectitic aggregates in mantle rocks (e.g. Godard and Martin, 2000; Förster et al., 2017).

Spinel-orthopyroxene (± clinopyroxene) symplectites are an important feature of the New Caledonia residual peridotites. Their presence in the Massif du Sud harzburgites (Yaté area) has been previously reported by Pirard et al.

(2013). These authors suggested that spinel-pyroxene symplectites originated from a precursor garnet phase, explaining the Cr-rich nature of these clusters as inherited from homogenization of spinel compositions with the surrounding peridotite (Pirard et al., 2013). However, a detailed investigation of these structures is lacking, thus the genesis of the spinel-pyroxene clusters still remains an open issue.

In this work, we describe the symplectitic intergrowths occurring in harzburgites coming from two different peridotitic massifs: Kopeto, central massif and Yaté, Massif du Sud. Petrographic and major element chemical investigation of these spinel-pyroxene clusters has been carried out in order to constrain their origin during the harzburgite evolution.

GEOLOGICAL AND PETROLOGICAL BACKGROUND

New Caledonia is a NW-SE elongated island located in the SW Pacific region among the New Hebrides Arc (Vanuatu) and the eastern Australian margin.

The main island of New Caledonia, named Grande Terre, includes an association of volcanic, sedimentary and metamorphic terranes of Permian to Miocene age (Aitchison et al., 1995; Cluzel et al., 2001; 2012, Lagabrielle et al., 2013). These terranes were assembled during two major tectonic episodes: 1) a Permian to Early Cretaceous W-dipping subduction related to the eastern Gondwana active margin and 2) an Eocene NE-dipping subduction eventually resulting in the obduction of the ophiolitic units. Both tectonic events were characterized by high-pressure (HP-LT) metamorphism and were separated by a phase of oceanic spreading, related to a Late Cretaceous-Paleocene marginal basin formation.

Following Cluzel et al. (2001) the Island can be subdivided into four main geological domains: (i) the autochthonous units, including a pre-Late Cretaceous basement and its late Coniacian to Late Eocene sedimentary cover, (ii) the Eocene HP-LT metamorphic belt (iii) the dominantly basaltic Poya Terrane and (iv) a large sheet of obducted mantle rocks referred as to the Peridotite Nappe (Avias, 1967).

The Peridotite Nappe represents the obducted oceanic lithosphere belonging to the South Loyalty Basin (Collot et al., 1987), which recorded the Late Cretaceous-Paleocene marginal basin formation followed by Eocene convergence and obduction in a NE-dipping subduction zone (Cluzel et al., 1998).

The Peridotite Nappe represents one of the largest and best-preserved mantle exposure worldwide, extending approximately for 8000 km^2 and reaching a maximum thickness of 2500 m. Several phases of erosion left remnants of tectonic klippen spread along the west coast, some smaller lenses in the central ridge and a larger unit ("Massif du Sud"), which dominates the southern part of the island. The Peridotite Nappe is bounded at its lower limit by a 20 to 200 m thick highly-sheared serpentinite sole related to the obduction process (Quesnel et al., 2016).

The ultramafic Peridotite Nappe is dominantly formed of mantle rocks, mostly harzburgites and minor lherzolites (e.g. Ulrich et al., 2010; Secchiari et al., 2016), locally overlain by mafic-ultramafic lithologies (Prinzhofer, 1981). The mafic-ultramafic sequence is composed by dunites, wehrlites, rare pyroxenites and gabbroic rocks. The formation of this sequence has been ascribed to migration and accumulation of primitive ultra-depleted magma batches in the lower crust and Moho transition zone of a nascent arc (Marchesi et al.,

2009; Pirard et al., 2013; Secchiari et al., 2018).

Notably, the upper oceanic crust is completely missing in the ophiolite (Prinzhofer et al., 1980; Prinzhofer and Allègre, 1985). According to Cluzel et al. (2001) the crustal sequence was most likely eroded or tectonically detached before, during and/or after obduction. However, basaltic rocks with different geochemical features, ranging from back-arc basin basalts (BABB) to E-MORB compositions (e.g. Cluzel et al. 2001), can be found in the Poya Terrane, which tectonically underlies the Peridotite Nappe.

Clinoenstatite-bearing boninitic lava blocks of Early Eocene age are found in the serpentinite sole of the Peridotite Nappe. The origin of the boninites has been attributed by Cluzel et al. (2016) to hydrous melting of a depleted mantle source re-enriched by slab melts.

Recent geochemical works focused on the peridotitic lithologies have significantly improved our knowledge on the ophiolitic complex (e.g. Marchesi et al., 2009; Ulrich et al., 2010; Pirard et al., 2013; Secchiari et al., submitted). The New Caledonia harzburgites are ultra-depleted rocks, as indicated by the complete lack of primary clinopyroxene (Prinzhofer and Allègre, 1985) and the exceedingly low trace element concentrations. According to Marchesi et al. (2009) and Ulrich et al. (2010), the evolution of the harzburgites was linked to the development of the Eocene subduction system, where high degree of fluid-assisted melting (up to 25%) occurred. A more complex evolution, starting from melting depletion to late stage metasomatism, has been reconstructed by Secchiari and coauthors (submitted). In this scenario, the harzburgites record a multi-stage history including melt extraction under dry conditions (15% degree of fractional melting of a DMM source), followed by hydrous melting in supra-subduction zone environment (up to 18% degree of fractional melting) and, finally, late stage metasomatism operated by slab-derived fluids bearing small fractions of dissolved silicate melt. This evolution was likely related to the onset of a rifting phase in a marginal basin and the following convergence after tectonic inversion.

PETROGRAPHY AND MINERAL CHEMISTRY

For this work we selected four samples of harzburgite from two localities: Kopeto, central massif and Yaté, Massif du Sud (see Fig. 1).

The harzburgites are low-strain tectonites showing porphyroclastic textures (Fig. 2a, b), locally grading into protomylonite. A protogranular texture has been observed for the sample YA1. Recrystallized domains exhibiting equigranular mosaic-type textures are commonly found in all the analyzed samples.

The main mineral assemblage consists of olivine (~ 75-85 vol%), orthopyroxene (~ 15-25 vol%) and spinel (< 1 vol%), while primary clinopyroxene is remarkably absent. Secondary phases include rare serpentine (YA1), chlorite and tremolitic amphibole, often in association with talc.

Olivine occurs as elongated and kinked porphyroclasts (Fig. 2a), defining a well-developed foliation in association with orthopyroxene and spinel. In the Kopeto samples olivine has high Mg# (0.909-0.933) coupled with low CaO concentrations (< 0.10 wt.%), while NiO contents ranges between 0.22-0.72 wt.%. In Yaté harzburgite, olivine shows a narrow range of values for Mg# (0.914-0.918), slightly higher CaO (up to 0.10 wt.%) and similar NiO concentrations (0.33-0.64 wt.%).
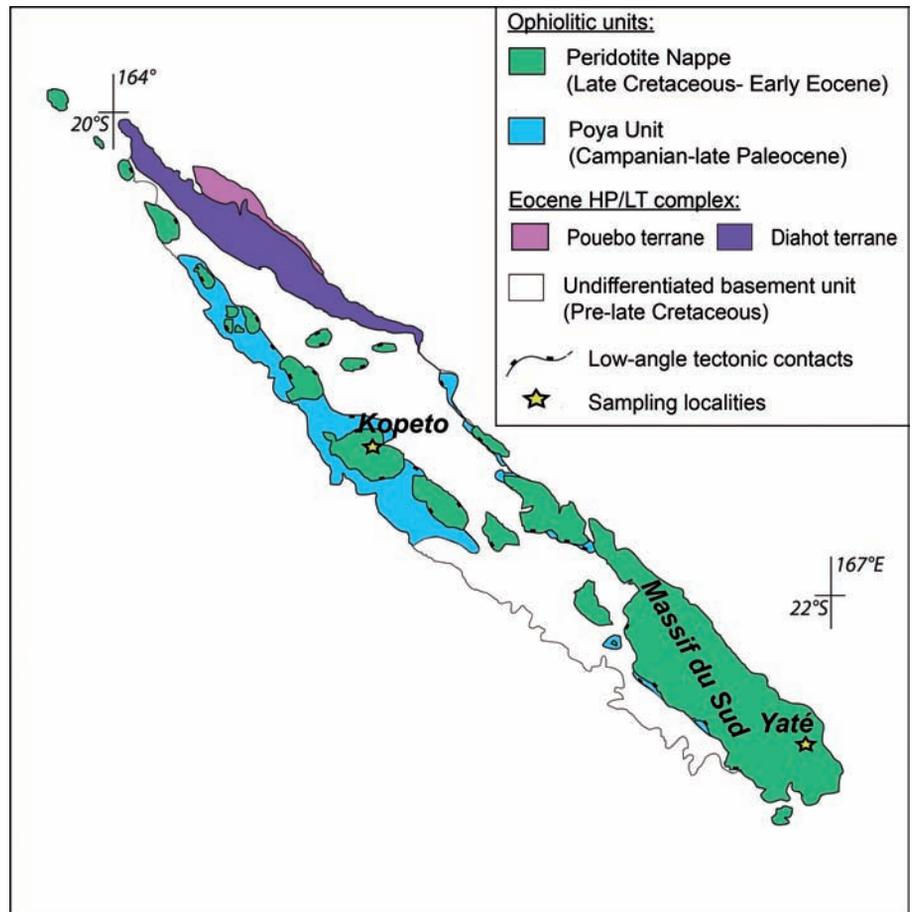
Fig. 1 - Simplified sketch map of New Caledonia showing the distribution of the Peridotite Nappe, Poya Terrane and autochtonous units. Stars represent main sampling locations of this study: Kopeto, central massif, coordinates: 21° 11′ 50.95′ S, 165° 04′ 31.45′ E) and Yaté, Massif du Sud, coordinates: 22° 09′ 25.2′ S, 166° 49′ 07.8′ E). Modified after Cluzel et al. (2012).

Brownish orthopyroxene appears as coarse-grained crystals (up to 2 mm in size, Fig. 2b), showing evidence of deformation (i.e. kink bands and undulous extinction) and exsolution lamellae of clinopyroxene. Orthopyroxene porphyroclasts frequently display irregular grain boundaries and embayments filled with undeformed olivine crystals (Fig. 2c). Small crystals of orthopyroxene are also found together with vermicular spinel, as the main component of the symplectitic intergrowths. Orthopyroxene is also present in the Kopeto samples as small, exsolution-free and undeformed crystals, in close association with thin films of secondary clinopyroxene (Fig. 2d).

Porphyroclastic orthopyroxene is enstatite with high Mg# (Table 1: 0.918-0.923 and 0.920-0.924, for Kopeto and Yaté samples, respectively). Al_2O_3 contents are low and cover the range between 1.76-2.73 wt.% (Kopeto) and 1.26-1.42 wt.% (Yaté). Cr_2O_3 contents vary between 0.66-1.12 wt.% and 0.53-0.76 wt.% for the two localities. Both Al_2O_3 and Cr_2O_3 display core-to-rim decreasing values. CaO concentrations of porphyroclast cores range between 0.98-1.49 wt.% and 0.86-1.03 wt.% for Kopeto and Yaté harzburgites. By contrast, metasomatic orthopyroxene has Al_2O_3 (0.88-1.12 wt.%), Cr_2O_3 (0.55-0.88 wt.%) and CaO-poor (0.31-0.56 wt.%) compositions, akin to metasomatic orthopyroxenes precipitated from slab-derived fluids (e.g. Arai and Ishimaru, 2008).

Symplectitic orthopyroxene shows Mg# values similar to porphyroclastic orthopyroxene (0.915-0.922 for Kopeto and 0.919-0.924 for Yaté). All the studied samples show lower Al_2O_3 contents compared to porphyroclastic orthopyroxene (1.21-2.19 wt.% for Kopeto and 0.80-1.20 wt.% for Yaté),

while Cr_2O_3 ranges between 0.41-0.74 wt.% and 0.45-0.59 wt.% for Kopeto and Yaté harzburgites, respectively. Core-to-rim decreasing concentrations are observed for Al_2O_3 in all the investigated samples, whereas Cr_2O_3 displays the opposite behaviour. CaO is relatively low and varies between 0.43-0.93 wt.% (Kopeto) and 0.50-0.62 wt.% (Yaté).

Small clinopyroxene crystals have been detected as secondary phase in some of the studied samples (KPT1, KPT5, YA1). Clinopyroxene can occur as rounded grains (c. 100 μm) in association with secondary orthopyroxene or as thin films around olivine porphyroclasts (Fig. 2d). Clinopyroxene crystals are sometimes also present in the symplectitic intergrowths (samples KPT1 and YA1).

Secondary clinopyroxene (Table 2) displays high Mg# values (0.944-0.950) and low Al_2O_3 and Cr_2O_3 contents (0.69-0.96 wt.% and 0.33-0.64 wt.%, respectively). Na_2O is generally below the detection limit (< 0.10 wt%) Symplectitic clinopyroxene exhibits slightly different major element composition compared to metasomatic clinopyroxene, showing higher Al_2O_3 for KPT1 (0.96-1.78 wt.%) or lower Al_2O_3 (0.44-0.52 wt.%) and higher Cr_2O_3 (0.66-0.68 wt.%) for YA1.

Chromian spinel occurs as reddish-dark brown crystals, showing rounded or holly leaf shape (Spl 1), or as symplectitic intergrowths (Spl 2) with orthopyroxene (± clinopyroxene). Spl 2 generally exhibits elliptical shapes with major axes size varying between ca 0.5-2.0 μm (Kopeto samples) or in the range of few tenths or hundred of mm (Yaté sample).

On the basis of Spl 2 morphology and geometric relationships among Spl 2 and the other mineral phases, the symplectites can be classified into two different sub-types:

Table 1- Representative orthopyroxene major element compositions (wt.%) of the New Caledonia harzburgites.

Sample	KPT1	KPT1	KPT1	KPT3	KPT3	KPT3	KPT3	KPT5	KPT5	KPT5	KPT5	YA1	YA1
Type	Pfc core	Pfc rim	Sec	Pfc core	Pfc rim	Nb	Sec	Pfc core	Pfc rim	Nb	Sec	Pfc core	Pfc rim
SiO_2	56.48	56.83	57.22	56.13	56.93	56.13	57.73	57.01	56.52	55.83	58.20	57.51	57.96
TiO_2	bdl	bdl	0.06	bdl	bdl	bdl	bdl	bdl	bdl	bdl	bdl	bdl	0.06
Al_2O_3	1.76	1.66	1.00	2.73	2.36	2.73	1.12	2.02	2.24	2.75	1.03	1.42	1.30
Cr_2O_3	0.70	0.65	0.83	1.12	0.81	1.12	0.88	0.66	0.73	1.08	0.55	0.76	0.60
FeO	5.41	5.22	5.37	5.32	5.16	5.32	4.99	5.05	5.47	5.27	4.97	5.01	5.34
MnO	0.00	0.23	0.19	0.13	0.12	0.13	0.15	0.17	0.16	0.19	0.11	0.09	0.16
MgO	34.22	34.22	35.42	33.58	33.72	33.58	35.11	34.00	33.87	33.14	34.90	34.32	34.42
CaO	1.49	1.39	0.56	0.98	0.89	0.98	0.31	1.00	0.77	0.95	0.32	0.90	0.84
Total	100.05	100.20	100.65	100.00	99.99	100.00	100.29	99.92	99.77	99.21	100.09	100.01	100.67
Mg#	0.919	0.921	0.922	0.918	0.921	0.918	0.926	0.923	0.917	0.918	0.926	0.924	0.920

Sample	KPT1	KPT1	KPT1	KPT3	KPT3	KPT3	KPT3	KPT3	KPT3	KPT5	KPT5	KPT5	KPT5	YA1	YA1
Type	Sympl	Sympl	Sympl	Sympl core	Sympl rim	Sympl core	Sympl rim	Sympl core	Sympl rim	Sympl core	Sympl rim	Sympl core	Sympl rim	Sympl	Sympl
SiO_2	57.01	56.40	56.97	57.57	57.58	56.68	57.07	57.49	57.73	56.54	56.83	57.75	57.45	58.60	58.69
TiO_2	bdl	0.14	0.02	bdl	bdl	bdl	bdl	bdl	bdl	bdl	bdl	bdl	bdl	0.02	bdl
Al_2O_3	1.21	1.47	1.08	1.81	1.50	2.19	1.36	1.58	1.12	1.98	1.56	1.56	1.34	0.81	0.80
Cr_2O_3	0.74	0.57	0.57	0.41	0.87	0.66	1.23	0.61	0.88	0.63	0.86	0.58	0.84	0.45	0.59
FeO	5.50	5.79	5.50	5.24	4.92	5.19	5.26	5.36	4.99	5.43	5.42	5.17	5.18	5.17	5.14
MnO	0.13	0.22	0.16	0.26	0.20	0.18	0.00	0.07	0.15	0.27	0.27	0.13	0.14	0.29	0.17
MgO	35.12	34.83	35.37	34.42	35.04	34.19	34.95	34.49	35.11	33.92	34.56	34.41	34.71	34.88	34.96
CaO	0.59	0.70	0.55	0.56	0.67	0.93	0.58	0.43	0.31	0.93	0.47	0.53	0.53	0.50	0.42
Total	100.29	100.11	100.22	100.27	100.78	100.01	100.46	100.03	100.29	99.71	99.97	100.13	100.19	100.72	100.76
Mg#	0.919	0.915	0.920	0.921	0.927	0.922	0.922	0.920	0.926	0.918	0.919	0.922	0.923	0.923	0.924

Bdl= below detection limit; Pfc= porpyroclast; Nb= neoblast; Sec= secondary; Sympl= symplectitic.
Major element mineral analyses were performed at the Dept. of Chemistry, Life Sciences and Environmental Sustainability in Parma using a JEOL-6400 electron microprobe equipped with a LINK-ISIS energy dispersive microanalytical system. The electron beam was produced at an accelerating voltage of 15 kV and probe current of 0.25 nA; both natural minerals and synthetic coumpounds were used as standards.
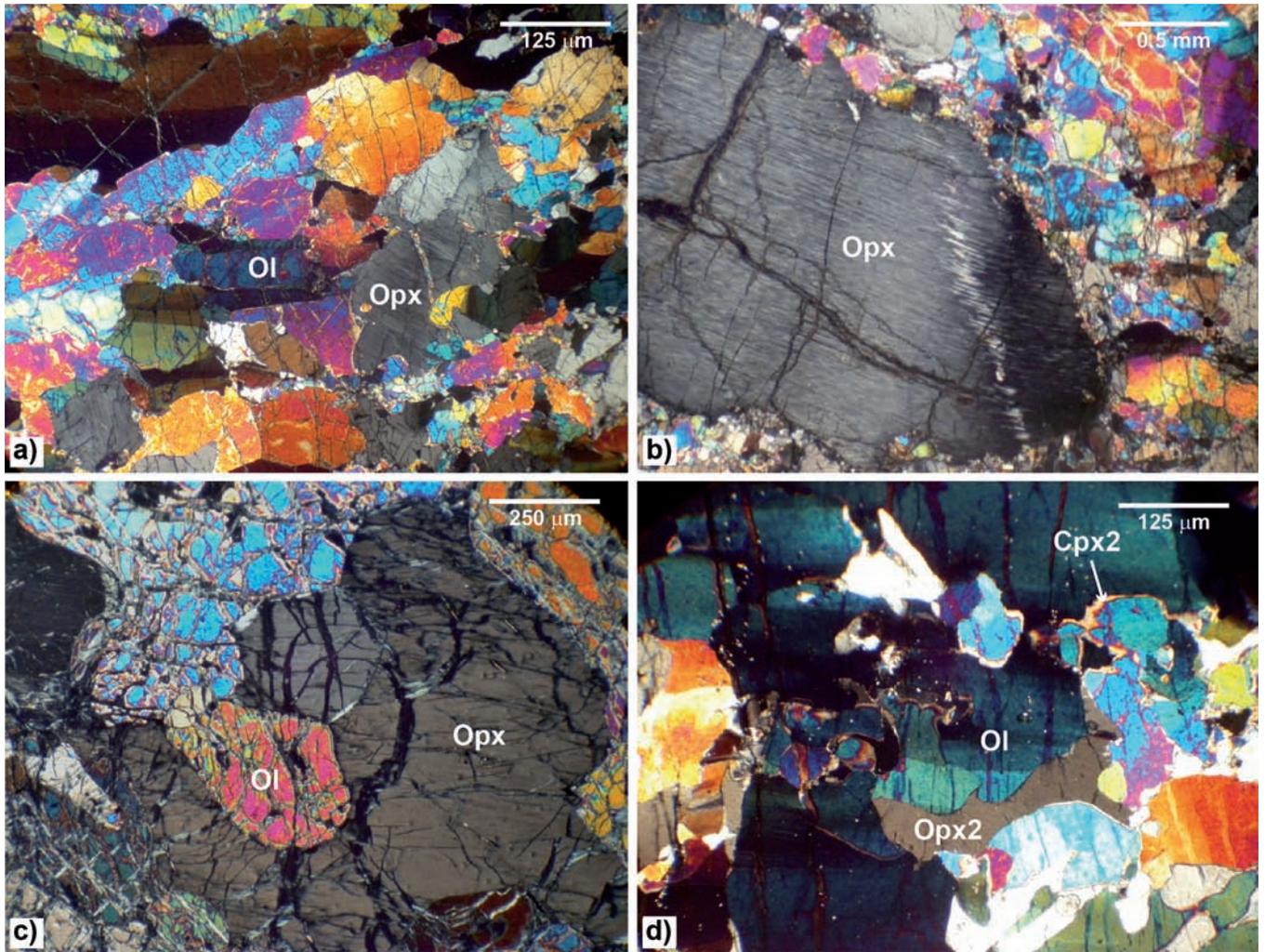
Fig. 2 - a) kinked and exsolved orthopyroxene and olivine porphyroclasts in foliated tectonite KPT1; b) strongly deformed orthopyroxene porphyroclast in olivine + orthopyroxene + spinel matrix (KPT3); c) orthopyroxene embayment filled with undeformed olivine (YA1); d) interstitial films of metasomatic clinopyroxene (Cpx2) and orthopyroxene (Opx2) developing along olivine porphyroclasts boundaries (KPT5).

Table 2 - Representative clinopyroxene major element compositions (wt.%) of the New Caledonia harzburgites.

Sample	KPT1	KPT1	KPT1	KPT1	YA1	YA1	YA1
Type	Sec	Sympl	Sympl	Sympl	Sec	Sympl	Sympl
SiO_2	53.59	53.57	53.59	53.10	54.27	54.20	54.16
TiO_2	0.10	bdl	0.10	bdl	0.05	0.05	bdl
Al_2O_3	0.96	1.46	0.96	1.78	0.69	0.52	0.44
Cr_2O_3	0.64	0.86	0.64	0.85	0.34	0.66	0.68
FeO	1.98	1.72	1.98	1.87	1.84	1.73	1.58
MnO	0.17	bdl	0.17	0.15	bdl	bdl	0.15
MgO	18.55	18.59	18.55	18.36	18.96	18.76	18.62
CaO	23.92	23.85	23.92	23.79	23.96	24.16	24.28
Na_2O	0.03	0.08	0.03	0.04	bdl	bdl	0.03
Total	99.94	100.12	99.94	99.94	100.11	100.08	99.95
Mg#	0.944	0.951	0.944	0.946	0.948	0.951	0.954

Bdl= below detection limit; Sec= secondary; Sympl= symplectitic.

1) Type-A (Kopeto samples: KPT1, KPT3, KPT5) consists of symplectites formed of Spl 2 with vermicular shapes (Fig. 3a) + orthopyroxene (± clinopyroxene). They generally grow along porphyroclastic olivine, which in turns displays evidence of chemical disequilibrium (i.e. irregular shapes and corroded profiles, Fig. 3b, c). Spl 2 generally seals small orthopyroxene (± clinopyroxene) grains, which may bear evidence of recrystallization (i.e. polygonal shapes and triple junctions, Fig. 3b);

2) Type-B (sample YA1, see Fig. 3d, e) encompasses symplectitic intergrowths with smaller size ("micro-symplectites", see Piccardo et al., 2007) composed of vermicular spinel + orthopyroxene (± clinopyroxene) forming "myrmekite-like", aggregates. Type-B symplectites develop
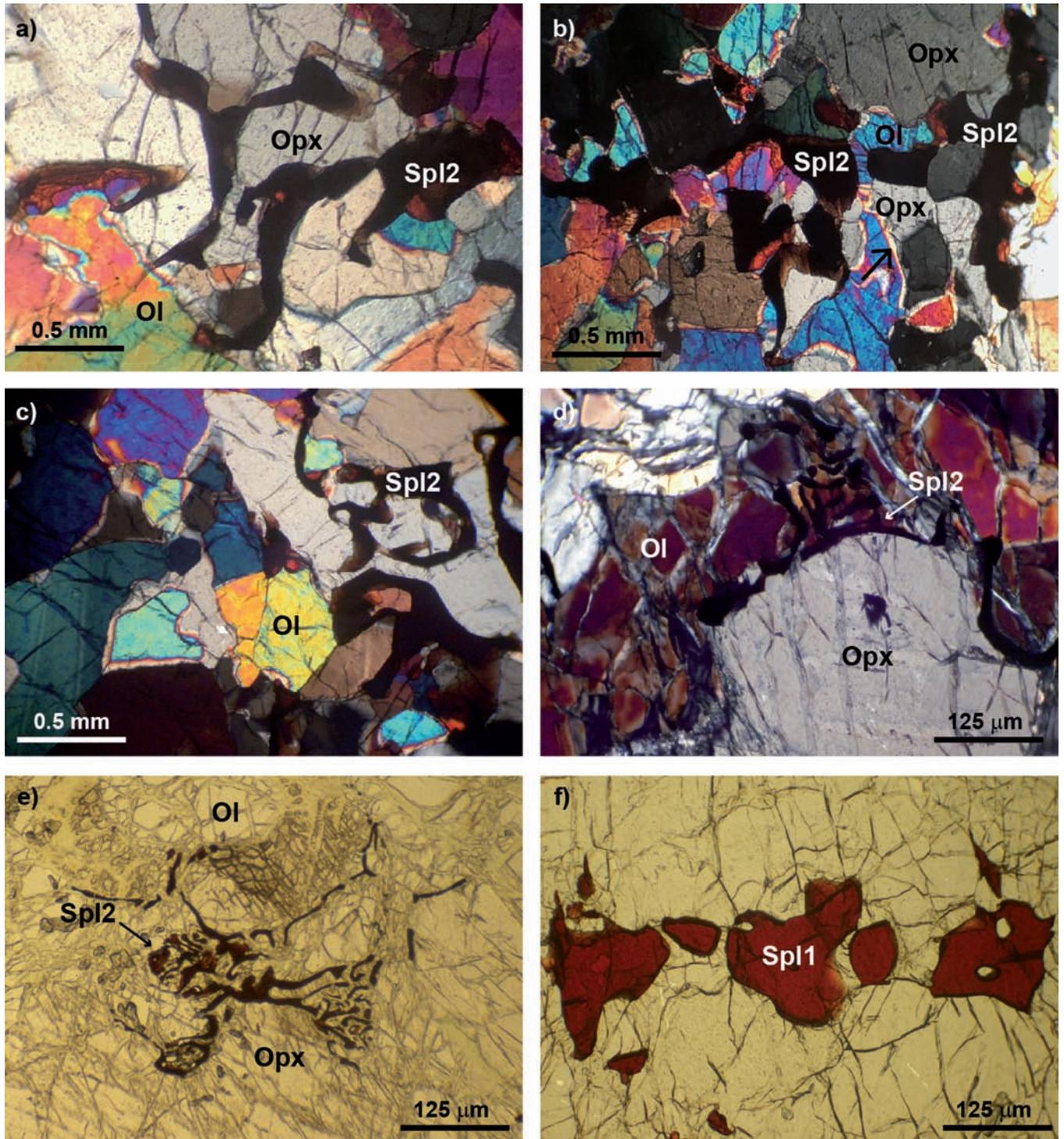
Fig. 3 - a) type-A spinel-orthopyroxene symplectitic intergrowths, crossed polars microphotograph, (KPT1 sample); b) spinel-orthopyroxene symplectitic structures in KPT3 harzburgite developing along corroded boundaries of olivine. Note minute symplectitic orthopyroxene (black arrow) showing evidence of recrystallization, i.e. straight boundaries and triple junctions; c) crossed polars image showing symplectitic spinel (Spl 2) growing along olivine porphyroclasts; d) type-B symplectites in YA1 sample; dark brown vermicular spinel (Spl 2) extends on olivine-orthopyroxene outline; e) spinel-orthopyroxene intergrowths developing along orthopyroxene porphyroclast (YA1); f) plane-polarized light microphotograph showing spinel of the porphyroclastic assemblage (Spl 1) in Kopeto harzburgites.

along grain boundaries on large orthopyroxene porphyroclasts or at orthopyroxene-olivine interface (Fig. 3d).

Spl 1 has homogeneous compositions within each sample, but exhibits some variability among harzburgites from the different localities (Table 3). Al_2O_3 varies between 24.55-30.48 wt.% (Kopeto) and 17.45-17.84 wt.% (Yaté) and shows core-to-rim increasing values. It is negatively correlated with Cr_2O_3 (41.45-47.99 wt.% for Kopeto and 52.44-52.95 wt.% for Yaté samples), which in turn displays core-to-rim decreasing values. Cr# (= Cr/(Cr+Al)) of Spl 1 in Kopeto (0.477-0.564) and Yaté samples (0.441-0.529) are remarkably high, in agreement with the highly refractory nature of these rocks.

Spl 2 is lower in Al_2O_3 compared to Spl 1 for KPT3 and KPT5 harzburgites (27.56-29.96 wt.%). By contrast, Spl 2 in YA1 sample exhibits slightly higher Al_2O_3 contents (18.17-20.79 wt.%) compared to Spl 1. Cr_2O_3 concentrations of Spl 2 ranges between 43.28-47.05 wt.% for Kopeto harzburgites and 49.28-51.70 wt.% for Yaté sample. Accordingly, the corresponding Cr# values overlap those of Spl 1 for Kopeto (0.483-0.554) or are shifted to slightly higher values (0.614-0.664) for Yaté (Fig. 4).

GEOTHERMOMETRY

In order to constrain the physical conditions of the symplectite formation, equilibrium temperatures have been computed by conventional thermometry on the basis of major element mineral composition. Ca-in-orthopyroxene (Brey and Kohler, 1990, i.e. T(BK)) and Ca-Mg exchange between clinopyroxene-orthopyroxene following Brey and Kohler (1990) and Taylor (1998) were applied to estimate the equilibrium temperatures of the symplectitic intergrowths for an assumed confining pressure of 1.5 GPa. The equilibrium temperature obtained by Ca-in-orthopyroxene formulation for the Kopeto and the Yaté harzburgites show core-to rim variation from 1030°C to 950-920°C, whereas the Yaté sample yields distinctly lower values (~ 880°C). Temperatures estimated using Ca-Mg exchange between clinopyroxene and orthopyroxene rims for Kopeto are ~860 °C, with a good agreement between Brey and Kohler (1990) and Taylor (1998) methods. The Yaté clinopyroxene-orthopyroxene T estimates yields

~ 810°C. In addition, single clinopyroxene thermometer of Nimis and Taylor (2000) provides consistent values of 865°C and 815°C for the two set of samples. Olivine-spinel geothermometry (Li et al., 1995) testifies cooling at T of 890-940°C for Kopeto and 865°C for the Yaté sample.

As a whole, all these temperatures are lower compared to those obtained for porphyroclastic orthopyroxene cores of the two localities (T (BK) = 1050-1165°C and 1025°C for Kopeto and Yaté, respectively). Notably lower temperature estimates have been also calculated for metasomatic orthopyroxenes from Kopeto (T (BK) = 810-920°C).

DISCUSSION

The petrological and compositional variability displayed by the New Caledonia spinel-pyroxene clusters suggest that various processes have to be invoked in the formation of type-A and type-B symplectites. In the next paragraphs the origin of the different symplectitic intergrowths in the New Caledonia harzburgites will be discussed.

Origin of type-A symplectites: Kopeto harzburgites

Type-A symplectites are characterized by elongated shapes, with vermicular spinel being irregularly spaced and showing different lengths, from ~ 0.5 up to 2 mm (Fig. 3a - c). These shapes are different compared to those observed, for instance, in Horoman or Tallante symplectites, which were interpreted as a textural heritage of pre-existing garnet. The latter, in fact, often form rounded fine grained aggregates hosted in large orthopyroxene porphyroclasts, where spinel occurs as tiny dispersed crystals (e.g. Takahashi, 2001; Morishita and Arai, 2003; Shimizu et al., 2008).

Type-A symplectites extend along porphyroclastic olivine showing evidence of chemical disequilibrium, as indicated by irregular symplectite-olivine contacts and corroded olivine profiles (see Fig. 3b, c). This suggests that Kopeto symplectites originated at the expense of olivine, which should represent the reactant mineral. Hence, such structures may possibly indicate the breakdown of a high-pressure stabilized garnet through the reaction: Olivine + Garnet → Clinopyroxene + Orthopyroxene + Spinel.
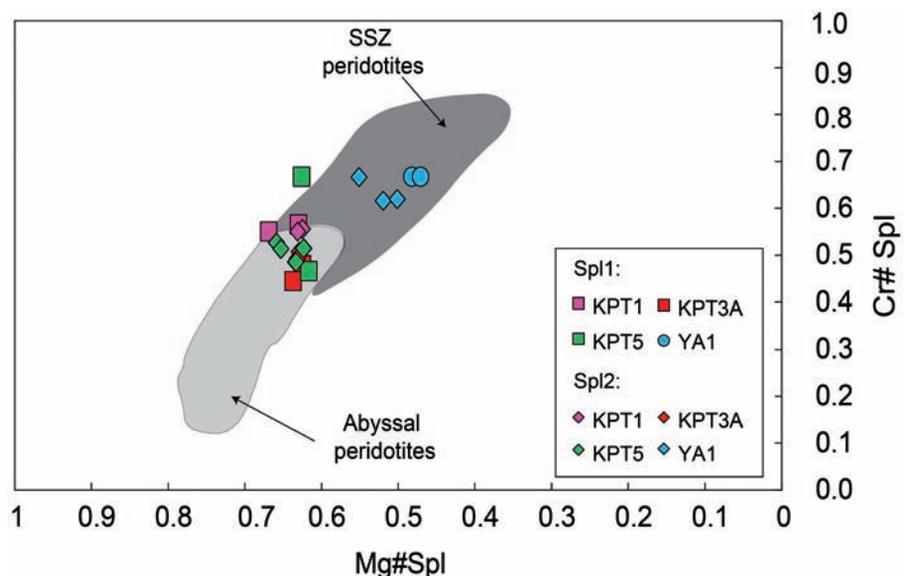
Fig. 4 - Compositional variations (Cr# vs. Mg#) of Spl 1 and Spl 2. Field for abyssal and fore-arc peridotites are taken from Dick and Bullen (1984) and Ishii et al. (1992), respectively.

Table 3 - Representative spinel major element compositions (wt.%) of the New Caledonia harzburgites.

Sample Type	KPT1 core	KPT1 rim	KPT3A core	KPT3A rim	KPT5 core	KPT5 rim	YA1 core	YA1 rim
V_2O_5	bdl	bdl	0.28	0.25	bdl	bdl	bdl	bdl
SiO_2	bdl	bdl	bdl	bdl	0.02	0.35	0.32	0.29
TiO_2	bdl	bdl	bdl	bdl	bdl	bdl	bdl	bdl
Al_2O_3	24.55	25.46	30.48	32.75	28.81	30.63	17.84	17.71
Cr_2O_3	47.31	46.18	41.45	38.81	42.98	40.71	52.95	52.52
FeO	13.99	13.15	13.68	13.59	14.09	13.19	19.14	19.72
MnO	0.61	0.50	0.59	0.38	0.48	0.46	0.04	0.30
MgO	13.07	14.29	12.52	13.04	12.51	13.29	10.38	10.19
CoO	bdl	bdl	0.13	0.26	0.02	0.45	bdl	bdl
Total	99.52	99.58	99.13	99.08	98.90	99.08	100.66	100.71
Mg#	0.625	0.660	0.620	0.631	0.613	0.621	0.491	0.481
Cr#	0.564	0.549	0.477	0.443	0.500	0.464	0.666	0.665

Sample Type	KPT1 Sympl	KPT3 Sympl core	KPT3 Sympl rim	KPT3 Sympl core	KPT3 Sympl rim	KPT5 Sympl core	KPT5 Sympl rim	KPT5 Sympl core	KPT5 Sympl rim	YA1 Sympl	YA1 Sympl	YA1 Sympl
V_2O_5	bdl	0.33	0.41	bdl	bdl	0.33	0.41	bdl	bdl	bdl	bdl	bdl
SiO_2	bdl	0.23	0.23	0.25	0.34	0.23	0.23	0.25	0.34	0.28	0.26	0.22
TiO_2	0.03	bdl	bdl	bdl	bdl	bdl	bdl	bdl	bdl	bdl	bdl	0.03
Al_2O_3	25.42	27.96	29.96	27.56	28.37	27.96	29.96	27.56	28.37	20.79	18.17	20.44
Cr_2O_3	47.05	43.82	41.79	45.37	44.23	43.82	41.79	45.37	44.23	49.37	51.02	49.28
FeO	14.20	13.84	13.33	12.57	12.94	13.84	13.33	12.57	12.94	18.77	17.49	19.40
MnO	0.27	0.20	0.42	0.38	0.35	0.20	0.42	0.38	0.35	0.11	0.45	0.40
MgO	13.00	12.58	12.62	13.12	13.20	12.58	12.62	13.12	13.20	11.40	11.66	10.90
CoO	bdl	0.20	0.39	0.19	bdl	0.2	0.39	0.19	bdl	bdl	bdl	bdl
Total	99.96	99.16	99.15	99.44	99.43	99.16	99.15	99.44	99.43	100.71	99.05	100.66
Mg#	0.620	0.618	0.628	0.651	0.645	0.619	0.628	0.651	0.645	0.525	0.553	0.509
Cr#	0.554	0.513	0.483	0.525	0.511	0.513	0.483	0.525	0.511	0.614	0.664	0.618

Bdl- below detection limit; Pfc- porpyroclast; Nb- neoblast; Sympl- symplectitic.

In order to test this hypothesis, bulk major element compositions for two symplectitic domains in KPT3 and KPT5 samples have been calculated following the methods of Obata et al. (1997) and Morishita and Arai (2003). First, 2D modal proportions of the mineral phases present in the symplectitic intergrowths have been obtained through image analysis. After, bulk composition for each symplectitic domain has been computed by mass balance calculations. Then, the model garnet composition has been obtained by subtracting an adequate amount of olivine component (~ 14% for KPT3 and 5% for KPT5) from the composition of the bulk symplectites, until the rest approaches ideal garnet stoichiometry, i.e. the total cation numbers become eight for O = 12.

Bulk major element contents for the analyzed symplectites are reported in Table 4. As a whole, the calculated compositions are broadly similar to some sub-calcic Cr-pyrope garnets documented for deep mantle rocks and xenoliths (e.g. Griffin et al., 1999; Pearson et al., 2014). The occurrence of these garnets has been reported for relatively cold (T = 900-1100°C) sub-continental lithospheric mantle sampled beneath Archean terrains, in frequent association with diamond, at depths between ~ 130-180 km (e.g. Gurney and Switzer, 1973; Sobolev et al., 1973; Griffin et al., 1999)

However, some lines of evidence make a derivation from a Cr-pyrope garnet highly unlikely. First, the chemical formula calculated for the model garnet reveals stoichiometric deficiency for Si (see Table 4). Second, clinopyroxene does not occur in all the analyzed symplectites and, where present, is very scarce. Third, garnets with similar features have been exclusively documented in Archean cratonic mantle sections (Griffin et al., 1999), which is not consistent with the envisaged geodynamic scenario of the New Caledonia peridotites. In fact, these mantle rocks are believed to record relatively recent geological events affecting former convective mantle evolving from Cretaceous marginal rifting to the Eocene convergence (e.g. Aitchison et al., 1995; Cluzel et al., 2001; 2012).

Table 4 - Major-element compositions (wt.%) of bulk spinel-pyroxene clusters and calculated major-element compositions of the model garnet.

Sample Type	KPT3 Bulk	KPT3 Model grt	KPT5 Bulk	KPT5 Model grt
SiO_2	33.64	33.13	37.82	38.04
Al_2O_3	10.96	13.07	10.57	10.68
Cr_2O_3	18.46	18.89	14.92	15.08
FeO	8.37	8.64	7.90	8.00
MnO	0.18	0.20	0.23	0.23
MgO	28.34	25.44	28.01	27.17
CaO	0.56	0.58	0.57	0.41
Total	100.51	99.94	100.01	99.62
Cations p.f.u.				
Si		2.521		2.841
Al		1.172		0.941
Cr		1.136		0.890
Fe		0.550		0.500
Mn		0.013		0.015
Mg		2.885		3.024
Ca		0.047		0.033
Total		8.325		8.243

Modal proportions used for model garnet calculation are 42% Spl and 58% Opx (KPT3); 34% Spl and 66% Opx (KPT 5).

In addition, textural preservation of former garnet-bearing domains after two melting events seems quite unlikely. In particular, incongruent melting reactions in garnet peridotites (e.g. Walter, 1998) should lead to early garnet consumption at pressures compatible with the inferred geodynamic setting. Finally, REE geochemistry of the studied rock-types does not support a similar origin, as bulk rock REE fractionation is not indicative of melting in the garnet stability field (see Secchiari et al., submitted). We therefore exclude that the spinel-pyroxene clusters could bear witness of a pre-existing Cr-rich garnet in the New Caledonia mantle.

By contrast, the excellent preservation of these structures and their peripheral location along irregular or corroded olivine boundaries may be clues of a post-melting origin.

A remarkable feature of the Kopeto symplectites is represented by the very high modal concentration of symplectitic spinel (up to 36%) in these structures, in contrast with the low bulk abundances (< 1 vol%) of primary spinel in both symplectite-bearing and symplectite-free harzburgites. Such high modal proportions are not consistent with the melting history of the Kopeto harzburgites, as spinel is expected to be almost exhausted in a mantle residue that experienced the high melting degrees inferred for these rocks (Kinzler, 1997; Gaetani and Grove, 1998). Moreover, symplectitic spinel shows absolute larger sizes (up to 1-2 mm vs. few μm for primary spinel) and different shapes in the symplectitic domains compared to primary spinel. While primary spinel is often constituted by tiny, rounded or, more rarely, by holly leaf shaped crystals (Fig. 3f) located in intergranular position, symplectitic spinel bears vermicular or "fluidal", "magmatic" shapes growing along corroded olivine boundaries (Fig. 3b, c). The aforementioned observations hint that symplectitic spinel cannot represent a residual phase, but a rather a newly formed phase, possibly derived from a melt. Major element chemical variation displayed by symplectitic spinel, i.e. core-to-rim increasing Al_2O_3 and decreasing Cr_2O_3 values (see Table 3), are consistent with such an origin.

Remarkably, analogous structures have been recognized in modern abyssal peridotites and gabbroic rocks from arc setting, where their genesis has been related to melt-rock interactions (De Haas et al., 2002; Seyler et al., 2007; Suhr et al., 2008; Helmy et al., 2008).

In the investigated harzburgites, the crystallization of new orthopyroxene (+ Cr-spinel ± clinopyroxene) at the expense of olivine, requires that the melt involved in the symplectite-forming reaction was an orthopyroxene-saturated melt. Orthopyroxene saturation may be reached in olivine-saturated high-P partial melts that reacted during their ascent with host peridotites forming olivine at the expense of orthopyroxene, as frequently observed in abyssal and ophiolitic peridotites (e.g. Seyler et al., 2007; Piccardo et al., 2007; Rampone et al., 2008). However, considering the geodynamic setting of this study, a more realistic hypothesis may take into account relatively silica-rich, low-P hydrous melts formed by partial melting of a depleted peridotite, in equilibrium with a clinopyroxene-free residue. Interaction among the depleted harzburgite and SiO_2-saturated, hydrous melts in supra-subduction zone setting is in fact testified for the lithologies of this study by the frequent occurrence of Al_2O_3-, Cr_2O_3- and CaO-poor metasomatic orthopyroxene, associated with thin films of Al_2O_3-, Cr_2O_3- and Na_2O-poor clinopyroxene (Secchiari et al., submitted). Secondary pyroxene with similar major element chemical variations has been documented in arc peridotite xenoliths, where its presence has

been attributed to circulation of hydrous fluids containing small fractions of dissolved silicate melts (i.e. hydrous melts, Arai and Ishimaru, 2008).

Notably, in the New Caledonia ophiolite, the occurrence of high-SiO$_2$ melts with a depleted geochemical signature has been testified in the mafic-ultramafic cumulitic sequence overlying the tectonite harzburgites by Marchesi et al. (2009).

Estimates of crystallization temperatures indicate that the Kopeto symplectites formed in a relatively cold system, not exceeding 1030°C, before being partially re-equilibrated at T < 950°C. The general lack of exsolution textures in orthopyroxene prevents to infer a previous higher temperature stage, unless we assume that the tiny clinopyroxenes occurring in the symplectites are the product of unmixing from a CaO-rich orthopyroxene. The relatively low temperatures of formation for the symplectites, which are close to the wet peridotite solidus (e.g. see Schmidt and Poli, 1998), suggest that the symplectites may have either originated by interaction with a hydrous silicate melt or with a slab-derived (silicate-bearing?) aqueous fluid, as proposed for the genesis of replacive arc-related orthopyroxenites from the Solomon islands (Berly et al., 2006).

Notably, major element composition of ortho- and clinopyroxene occurring in the symplectites are comparable to those of interstitial, metasomatic pyroxenes (Table 1-2).

An alternative explanation may involve interaction between harzburgites and slab-derived adakitic melts, as supported by a recent experimental work of Corgne et al. (2018). According to these experiments, which were conducted at at 1.5 GPa, hydrous adakitic melts which have previously interacted with peridotite are predicted to produce olivine dissolution and crystallization of orthopyroxene + Cr-spinel + clinopyroxene at relatively low T (1000-1100°C).

Whether Type-A symplectites are the result of interaction with melts or slab-related fluid, such interaction did not significantly affect the whole rock budget in terms of trace element content, as no significant variations can be identified among symplectite-bearing and symplectite-free harzburgites (Secchiari et al., submitted). By contrast, a slight SiO$_2$ enrichment in whole rock has been recognized for two symplectite-bearing samples from the Kopeto, central massif (45.08-44.10 wt.% vs. 41.05-43.65 wt.% for the symplectite-free harzburgites). We propose that this feature may be the result of pyroxene addition by melt-or fluid-rock interaction.

Genesis of type-B symplectites: Yaté harzburgite

The sample from Yaté contains spinel-pyroxene symplectitic intergrowths displaying different texture, location and chemical composition compared to those belonging to the Kopeto harzburgites (Fig. 3). These features indicate that another process has to be taken into account in order to explain the genesis of type-B symplectites. In particular, Type-B symplectites develop as small (up to a few hundred of μm) "myrmekitic-like" or vermicular structures along the outer border of orthopyroxene porphyroclasts (Fig. 3e, f). No evidence of instability nor corroded profiles have been observed at symplectite-orthopyroxene boundaries. This suggests that spinel-pyroxene clusters do not derive from reactive melt percolation. By contrast, type-B symplectites resemble spinel-pyroxene symplectitic intergrowths reported for some Alpine peridotites (e.g. Piccardo et al., 2007; Rampone et al., 2008).

Major element chemical features can provide additional highlights in order to unravel the genesis of type-B symplectites. Orthopyroxene in YA1 harzburgite records systematic decrease in Al$_2$O$_3$ and Cr$_2$O$_3$ contents from porphyroclast cores to porphyroclast rims and small grains in the symplectitic aggregates (Table 1). Likewise, Mg# shows decreasing core-to-rim values, while symplectitic orthopyroxene bears similar Mg# values compared to those shown by porphyroclastic rims. Spl 1 displays major element variations consistent with those observed in porphyroclastic orthopyroxene, i.e. core-to-rim decreasing Al$_2$O$_3$, Cr$_2$O$_3$ and Mg# values. By contrast, Spl 2 is slightly enriched in Al$_2$O$_3$ compared to Spl 1 (see Table 3; 18.17-20.79 wt.% vs. 17.71-17.74 wt.%, respectively).

Similar major element chemical features have been documented in the spinel-pyroxene clusters of Monte Maggiore (Rampone et al., 2008), Erro Tobbio (Piccardo and Vissers, 2007) and South Lanzo peridotites (Piccardo et al., 2007) from the Alpine ophiolitic sequences. These structures have been interpreted as "cooling textures", formed from orthopyroxene with higher Al and Cr contents, which experienced significant cooling from asthenospheric conditions in the spinel stability field. Cooling resulted in unmixing of Cr-Mg-Tschermakitic components in form of spinel, due to decreased solubility of the Cr-Al component (CrMgTs, Klemme and O'Neill, 2000) and subsolidus Fe-Mg exchange reactions between pyroxenes and spinel at decreasing temperature.

The frequent occurrence of spinel-pyroxene micro-symplectites in the harzburgite from Yaté records cooling and re-equilibration at relatively low temperatures (< 900°C). We thus propose that the symplectitic stage registered by YA1 reflects post-melting cooling and re-equilibration during lithospheric incorporation.

CONCLUSIONS

An important feature of the New Caledonia harzburgites is represented by spinel-orthopyroxene (± clinopyroxene) symplectitic intergrowths. Such structures, despite being previously described for the New Caledonia harzburgites, have never been studied in detail. In this work, we have reported a textural, petrographical and major element chemical investigation of the spinel-pyroxene clusters occurring in the harzburgites from Kopeto, central massif and Yaté, Massif du Sud, areas.

Kopeto and Yaté symplectites, named type-A and type-B symplectites, display different shapes, textures and locations, indicating that different processes have to be taken into account for their genesis.

Textural features and bulk major element composition of type-A symplectites preclude an origin of these clusters as products of a pre-existing garnet phase. By contrast, their textural and compositional characteristics suggest derivation from melt- or fluid-rock interaction. Type-A symplectites originated from a relatively low temperature (T ~ 1030°C) post-melting event, in which localized interactions of the depleted harzburgite with orthopyroxene-saturated hydrous melts or slab-derived fluids generate spinel-pyroxene intergrowths through olivine dissolution.

Type-B symplectites occur as small ("micro-symplectites") spinel-pyroxene clusters growing on large orthopyroxene porphyroclasts. Yaté symplectites closely resemble in shape and major element contents some spinel-pyroxene

intergrowths documented in Alpine peridotites, i.e. Monte Maggiore, Erro Tobbio and South Lanzo peridotites. These structures record a low temperature (T < 900°C) re-equilibration of a Cr-Al richer, high-T, mantle orthopyroxene, resulting in unmixing of the CrMgTs component and precipitation of spinel-pyroxene symplectites.

The example of the New Caledonia symplectites indicates that spinel-pyroxene clusters in mantle rock-types can bear memory of geological processes that are not unambiguously testified by whole rock geochemistry.

ACKNOWLEDGEMENTS

REFERENCES

Aitchison J.C., Clarke L., Meffre S and Cluzel D., 1995. Eocene arc-continent collision in New Caledonia and implications for regional Southwest Pacific tectonic evolution. Geology, 23:161-164.

Arai S. and Ishimaru S., 2008. Insights into petrological characteristics of the lithosphere of mantle wedge beneath arcs through peridotite xenoliths: A review. J. Petrol., 49: 665-695.

Avias J., 1967. Overthrust structure of the main ultrabasic New Caledonian massives. Tectonophysics, 4: 531-541.

Berly T.J., Hermann J., Arculus R.J. and Lapierre H., 2006. Supra-subduction Zone pyroxenites from San Jorge and Santa Isabel (Solomon Islands). J. Petrol. 47: 1531-1555.

Brey G.P. and Kohler T., 1990. Geothermobarometry in four-phase lherzolites II. New thermobarometers, and practical assessment of existing thermobarometers. J. Petrol., 31: 1353-1378.

Cluzel D., Aitchison J.C. and Picard C., 2001. Tectonic accretion and underplating of mafic terranes in the Late Eocene intraoceanic fore-arc of New Caledonia (Southwest Pacific): geodynamic implications. Tectonophysics, 340: 23-59.

Cluzel D., Chiron D. and Courme M.D., 1998. Discordance de l'Eocène supérieur et événements pré-obduction en Nouvelle-Calédonie (Pacifique Sud-Ouest). C.R. Acad. Sci. Série 2, Sci. Terre Planets, 327: 485-491.

Cluzel D., Maurizot P., Collot J. and Sevin B., 2012. An outline of the geology of New Caledonia from Permian - Mesozoic Southeast Gondwanaland active margin to Cenozoic obduction and supergene evolution. Episodes, 35: 72-86.

Cluzel D., Ulrich M., Jourdan F., Meffre S., Paquette J.-L., Audet M.-A., Secchiari A. and Maurizot P., 2016. Early Eocene clinoenstatite boninite and boninite-series dikes of the ophiolite of New Caledonia; a witness of slab-derived enrichment of the mantle wedge in a nascent volcanic arc. Lithos, 260: 429-442.

Collot J.Y., Malahoff A., Recy J., Latham G. and Missegue F., 1987. Overthrust emplacement of New Caledonia Ophiolite: Geophysical evidence. Tectonics, 6: 215-232.

Corgne A., Schilling M.E., Grégoire M. and Langlade J., 2018. Experimental constraints on metasomatism of mantle wedge peridotites by hybridized adakitic melts. Lithos, 308-309: 213-226.

De Haas G.-J.L., Nijland T.G., Valbracht P.J., Maijer C., Verschure R. and Andersen T., 2002. Magmatic versus metamorphic origin of olivine-plagioclase coronas. Contrib. Mineral. Petrol., 143: 537-550.

Dick H.J.B. and Bullen T., 1984. Chromian spinel as a petrogenetic indicator in abyssal and alpine-type peridotites and spatially associated lavas. Contrib. Mineral. Petrol., 86: 54-76.

Field S.W. and Haggerty S.E., 1994. Symplectites in upper mantle peridotites: Development and implications for the growth of subsolidus garnet, pyroxene and spinel. Contrib. Mineral. Petrol., 118: 138-156.

Förster B., Braga R., Aulbach S., Lo Pò D., Bargossi G.M. and Mair V., 2017. A petrographic study of carbonate phases in the Ulten Zone ultramafic rocks: insights into carbonation in the mantle wedge and exhumation-related decarbonation. Ofioliti, 42: 105-127.

Gaetani G.A. and Grove T.L., 1998. The influence of water on melting of mantle peridotite. Contrib. Mineral. Petrol., 131: 323-346.

Godard M. and Martin S., 2000. Petrogenesis of kelyphites in garnet peridotites: a case study from the Ulten Zone, Italian Alps. J. Geodyn., 30: 117-145.

Godard M., Lagabrielle Y., Alard O. and Harvey J., 2008. Geochemistry of the highly depleted peridotites drilled at ODP Sites 1272 and 1274 (Fifteen-Twenty Fracture Zone, Mid-Atlantic Ridge): Implications for mantle dynamics beneath a slow spreading ridge. Earth Planet. Sci. Lett., 267: 410-425.

Griffin W.L., Fisher N.I., Friedman J., Ryan C.G. and O'Reilly S.Y., 1999. Cr-Pyrope garnets in the lithospheric mantle. J. Petrol., 40: 679-704.

Gurney J.J. and Switzer G.S., 1973. The discovery of garnets closely related to diamonds in the Finsch pipe, South Africa. Contrib. Mineral. Petrol., 39: 103-116.

Helmy H.M., Yoshikawa M., Shibata T., Arai S. and Tamura A., 2008. Corona structure from arc mafic-ultramafic cumulates: The role and chemical characteristics of late-magmatic hydrous liquids. J. Mineral. Petrol. Sci., 103: 333-344.

Ishii T., Robinson P.T., Mackawa H. and Fiske R., 1992. Petrological studies of peridotites from diapiric serpentinite seamounts in the Izu-Ogazawara-Mariana forearc, LEG 125. Proc. O.D.P. Sci. Results, 125: 445-485.

Kinzler R.J., 1997. Melting of mantle peridotite at pressures approaching the spinel to garnet transition: Application to mid-ocean ridge basalt petrogenesis. J. Geophys. Res., 102: 853-874.

Klemme S. and O'Neill H.S.C., 2000. The effect of Cr on the solubility of Al in orthopyroxene: experiments and thermodynamic modelling. Contrib. Mineral. Petrol., 140: 84-98.

Lagabrielle Y., Chauvet A., Ulrich M. and Guillot S., 2013. Passive obduction and gravity-driven emplacement of large ophiolitic sheets: The New Caledonia ophiolite (SW Pacific) as a case study? Bull. Soc. Géol. Fr., 184: 545-556.

Li J., Kornprobst J., Vielzeuf D. and Fabriès J., 1995. An improved experimental calibration of the olivine-spinel geothermometer. Chin. J. Geochem., 14: 68-77.

Marchesi C., Garrido C.J., Godard M., Belley F. and Ferré E., 2009. Migration and accumulation of ultra-depleted subduction-related melts in the Massif du Sud ophiolite (New Caledonia). Chem. Geol., 266: 171-186.

Medaris L.G., Fournelle J.H., Wang H.F. and Jelinek E., 1997. Thermobarometry and reconstructed chemical compositions of spinel-pyroxene symplectites: Evidence for pre-existing garnet in lherzolite xenoliths from Czech Neogene lavas. Russ. Geol. Geophys., 38: 277-286.

Morishita T. and Arai S., 2003. Evolution of spinel-pyroxene symplectite in spinel-lherzolites from the Horoman Complex, Japan. Contrib. Mineral. Petrol., 144: 509-522.

Nimis P. and Taylor W.R., 2000. Single clinopyroxene thermobarometry for garnet peridotites. Part I. Calibration and testing of a Cr-in-Cpx barometer and an enstatite-in-Cpx thermometer. Contrib. Mineral. Petrol., 139: 541-554.

Obata M., Morishita R. and Tanaka K., 1997. The microstructure of pyroxene-spinel symplectite from the Horoman peridotite and its formation processes. Mem .Geol. Soc. Jpn., 47: 163-171.

Pearson D.G., Canil D. and Shirey S.B., 2014. Mantle samples included in volcanic rocks: Xenoliths and diamonds. Treatise on Geochemistry (2nd ed.), 3 (5), p. 169-253.

Piccardo G.B. and Vissers R.L.M., 2007. The pre-oceanic evolution of the Erro-Tobbio peridotite (Voltri Massif, Ligurian Alps, Italy). J. Geodyn., 43: 417-449.

42

Piccardo G.B., Zanetti A. and Müntener O., 2007. Melt/peridotite interaction in the Southern Lanzo peridotite: Field, textural and geochemical evidence. Lithos, 94: 181-209.

Pirard C., Hermann J. and O'Neill H.S.C., 2013. Petrology and geochemistry of the crust-mantle boundary in a nascent arc, Massif du Sud Ophiolite, New Caledonia, SW Pacific. J. Petrol., 54: 1759-1792.

Prinzhofer A., 1981. Structure et pétrologie d'un cortège ophiolitique: le Massif du Sud (Nouvelle Calédonie). La transition manteau-croûte en milieu océanique. École nationale supérieure des mines (Paris), Thesis, 175 pp.

Prinzhofer, A. and Allègre C., 1985. Residual peridotites and the mechanisms of partial melting. Earth Planet. Sci. Lett., 74: 251-265.

Prinzhofer A., Nicolas A., Cassard D., Moutte J., Leblanc M., Paris J.P. and Rabinovitch M., 1980. Structures in the New Caledonia peridotites-gabbros: Implications for oceanic mantle and crust. Tectonophysics, 69: 85-112.

Quesnel B., Gautier P., Cathelineau M., Boulvais P., Couteau C. and Drouillet M., 2016. The internal deformation of the Peridotite Nappe of New Caledonia: A structural study of serpentine-bearing faults and shear zones in the Koniambo Massif. J. Struct. Geol., 85: 51-67.

Rampone E., Piccardo G.B. and Hofmann A.W., 2008. Multi-stage melt-rock interaction in the Mt. Maggiore (Corsica, France) ophiolitic peridotites: microstructural and geochemical evidence. Contrib. Mineral. Petrol., 156: 453-475.

Rampone E., Vissers R.L.M., Poggio M., Scambelluri M. and Zanetti A., 2009. Melt migration and intrusion during exhumation of the Alboran lithosphere: the Tallante mantle xenolith record (Betic Cordillera, SE Spain). J. Petrol., 51: 295-325.

Schmidt M.W. and Poli S., 1998. Experimentally based water budgets for dehydrating slabs and consequences for arc magma generation. Earth Planet. Sci. Lett., 163: 361-379.

Secchiari A., Montanini A., Bosch D., Macera P. and Cluzel D., 2016. Melt extraction and enrichment processes in the New Caledonia lherzolites: evidence from geochemical and Sr-Nd isotope data. Lithos, 260: 28-43.

Secchiari A., Montanini A., Bosch D., Macera M. and Cluzel D., 2018. The contrasting geochemical message from the New Caledonia gabbronorites: insights on depletion and contamination processes of the sub-arc mantle in a nascent arc setting. Contrib. Mineral. Petrol., 173: 66.

Secchiari A., Montanini A., Bosch D., Macera M. and Cluzel D., Submitted. Sr-Nd-Pb and trace element systematics of the New Caledonia harzburgites: tracking source depletion and contamination processes in SSZ setting. Geosci. Front., Ophiolites, Spec. Iss.

Seyler M., Lorand J.-P., Dick H.J.B. and Drouin M., 2007. Pervasive melt percolation reactions in ultra-depleted refractory harzburgites at the Mid-Atlantic Ridge, 15° 20′N: ODP Hole 1274A. Contrib. Mineral. Petrol., 153: 303-319.

Shimizu Y., Arai S., Morishita T. and Ishida Y., 2008. Origin and significance of spinel-pyroxene symplectite in lherzolite xenoliths from Tallante, SE Spain. Mineral. Petrol., 94: 27-43.

Smith D., 1977. The origin and interpretation of spinel-pyroxene clusters in peridotite. J. Geol., 85: 476-482.

Sobolev N.V., Lavrent'ev Y.G., Pokhilenko N.P. and Usova L.V., 1973. Chrome-rich garnets from the kimberlites of Yakutia and their parageneses. Contrib. Mineral. Petrol., 40: 39-52.

Suhr G., Kelemen P. and Paulick H., 2008. Microstructures in Hole 1274A peridotites, O.D.P. Leg 209, Mid-Atlantic Ridge: Tracking the fate of melts percolating in peridotite as the lithosphere is intercepted. Geochem. Geophys. Geosyst., 9 (3), p. Q03012, 10.1029/2007GC001726.

Takahashi N., 2001. Origin of plagioclase lherzolite from the Nikanbetsu Peridotite Complex, Hokkaido, Northern Japan: Implications for incipient melt migration and segregation in the partially molten upper mantle. J. Petrol., 42: 39-54.

Taylor R.W., 1998. An experimental test of some geothermometer and geobarometer formulations for upper mantle peridotites withapplication to the thermobarometry of fertile lherzolite and garnetwebsterite. N. Jahrb. Mineral. Abhandl., 172: 381-408.

Ulrich M., Picard C., Guillot S., Chauvel C., Cluzel D. and Meffre S., 2010. Multiple melting stages and refertilization as indicators for ridge to subduction formation: the New Caledonia ophiolite. Lithos, 115: 223-236.

Vannucci R., Shimizu N., Piccardo G.B., Ottolini L. and Bottazzi P., 1993. Distribution of trace elements during breakdown of mantle garnet: an example from Zabargad. Contrib. Mineral. Petrol., 113: 437-449.

Vernon R.H., 2004. A practical guide to rock microstructure. Cambridge Univ. Press, 606 pp.

Walter M.J., 1998. Melting of garnet peridotite and the origin of komatiite and depleted lithosphere. J. Petrol., 39: 2-60.